Hyper-Raman study of Li-induced polarization clusters in $K_{1-x}Li_xTaO_3$

1995 J. Phys.: Condens. Matter 7 5913

(http://iopscience.iop.org/0953-8984/7/29/018)

J. Phys.: Condens. Matter 7 (1995) 5913–5929. Printed in the UK

Hyper-Raman study of Li-induced polarization clusters in $K_{1-x}Li_xTaO_3$

H Vogt

Max-Planck-Institut für Festkörperforschung, Heisenbergstrasse 1, D-70569 Stuttgart, Germany

Received 6 April 1995

Abstract. The low-frequency hyper-Raman spectrum of $K_{1-x}Li_xTaO_3$ (x = 0.011, 0.016, and 0.036) is measured as a function of temperature between 10 and 200 K. At each Li concentration x and temperature T, the spectrum in the wavenumber range below 150 cm^{-1} is adequately described by the sum of a damped harmonic oscillator lineshape and a central δ function representing the soft-mode and hyper-Rayleigh scattering, respectively. The x and T dependence of the hyper-Rayleigh intensity $I_{HRL}(x, T)$ reflects the growth and coalescence of polarization clusters induced in the incipiently unstable host lattice by the off-centre displacements of the Li ions. The concept of a cluster coalescence temperature $T_{cc}(x)$ is introduced and verified for $I_{HRL}(x, T)$. From the increase of $I_{HRL}(x, T)$ between $T_{cc}(x)$ and 10 K, the low-temperature limit of the dipolar correlation radius is estimated. While $I_{HRL}(x, T)$ is a smooth and single-valued function of temperature for $x = 0.011$ and 0.016, it exhibits a thermal hysteresis loop with rather steep edges for $x = 0.036$, in accordance with a previous conjecture that the condensation of the Li subsystem changes its character at a crossover concentration around 0.022. In contrast to $I_{HRL}(x, T)$, the soft-mode frequency $\Omega_0(x, T)$ turns out to be insensitive to the coalescence of polarization clusters because it monitors quadrupolar rather than dipolar correlations. Up to $x = 0.036$, the Li-induced increase of the soft-mode damping constant $\gamma(x, T)$ cannot be explained in terms of an unresolved soft-mode splitting due to the tetragonal symmetry of the polarization clusters. Instead, the influence of symmetry reduction and disorder on the selection rules of multiphonon damping processes has to be considered. As in $I_{HRL}(x, T)$, new features are observed in $\gamma(x, T)$ when passing from $x = 0.016$ to $x = 0.036$.

1. Introduction

For about two decades the solid solution $K_{1-x}Li_xTaO_3$ (KLT) has attracted much interest because it seems to be the prototype material for studying a dilute random site electric dipole system embedded in a highly polarizable host lattice [1, 2]. The dipoles arise from the off-centre displacements of the Li impurities. The ionic radii of K^+ and Li^+ differing by a factor of almost two, the Li ions cannot match the centrosymmetric lattice sites of the K ions they substitute for. Instead, they are shifted along the ⟨100⟩ directions by an amount δ evaluations of which range from 0.64 Å [3] to 1.6 Å [4]. At elevated temperatures the Li ions are thermally activated to hop between the six equivalent off-centre positions permitted by the cubic overall symmetry of the crystal, the potential barrier of a $\pi/2$ flip being about 86 meV [5]. No variations of δ with temperature and Li concentration have been reported, except for an early conjecture that a decrease of δ with rising temperature may explain the weakening of impurity-induced first-order Raman features [6].

At first sight, the electrostatic interaction between the Li dipoles appears to be perfectly screened by the large dielectric constant of the $KTaO_3$ matrix, reaching values around 4400

0953-8984/95/295913+17$19.50

in the low-temperature limit. It is well known, however, that dielectric screening always competes with dielectric enhancement of the effective or external dipole moment defined by the force the dipole exerts on a distant charge in the dielectric [7]. In the simplest approximation, the effective dipole moment p^* is given by

$$p^* = \tfrac{1}{3}[\varepsilon(0) + 2]\, p_0 \tag{1}$$

where $\varepsilon(0)$ is the static dielectric constant of the host material and p_0 the dipole moment in vacuum. Equation (1) suggests the idea that each Li ion is surrounded by a polarization cluster the total dipole moment p^* of which exceeds the bare Li dipole moment $p_{Li} = e\delta$ at its centre by up to three orders of magnitude. It is not surprising that detailed model calculations and experiments have shown that equation (1) needs to be modified because it refers to idealized conditions hardly met in KLT.

According to the polarizable point charge model of van der Klink and Khanna [8], the dipole moment of a single off-centre Li ion almost cancels itself by inducing a cluster of opposite dipole moments in its environment. Enhancement instead of screening, i.e., $(p^*/p_{Li}) > 1$, is predicted by a nonlinear shell model calculation [9]. It is also evidenced by the magnitude of the Li-induced dispersion step [10] and by the remanent or electret polarization observed in electric-field-cooled samples at low temperatures ($T \leqslant 20$ K) [11]. In contrast to equation (1), however, enhancement factors p^*/p_{Li} only up to 25 have been reported. No agreement has been achieved about the temperature dependence of p^*/p_{Li} and the size of a single isolated polarization cluster. In view of the incipient instability of the host lattice with respect to the displacement pattern of the soft mode, one expects that both quantities increase with decreasing temperature [1, 12]. Nevertheless, just the opposite behaviour, i.e., a shrinkage of the polarization cluster on cooling, results from the model calculation of Stachiotti *et al* [13].

For all Li concentrations x investigated so far, the Li dipoles and their polarization clusters are found to interact and condense to a new phase at sufficiently low temperatures. Depending on x, this phase exhibits features of an orientational glass or of a fine-grained composite of ferroelectric domains still lacking any macroscopic spontaneous polarization under zero-field conditions. The extent to which KLT may be referred to as a dielectric analogue of a spin glass or as a partially ordered ferroelectric with dipole correlations on the mesoscopic length scale is still a matter of some controversy [1, 2, 14].

From birefringence data Kleemann *et al* [15] have inferred the boundary between low-temperature glass-type and ferroelectric-type states to lie at a crossover concentration x_c around 0.022. For $x < x_c$, KLT should freeze like a glass at a glass transition temperature $T_g < 40$ K, whereas for $x > x_c$, KLT should undergo a somewhat rounded first-order structural phase transition to a polydomain ferroelectric at a Curie temperature $T_C > 40$ K. A change of the transition character around x_c has been confirmed by subsequent second-harmonic generation (SHG), Raman, and dielectric studies [16–18, 20]. In accordance with the present understanding of a glass transition, evidence has been reported that the low-frequency tail of the spectrum of hopping rates involved in the collective dielectric response of the Li dipole system tends to a finite zero-frequency value at T_g for $x < x_c$ [19]. In contrast to the concept of a glass, however, anomalies in the temperature dependence of ultrasonic attenuation and velocity observed even for $x < x_c$ have been considered as indication of a structural transformation, albeit on a restricted length scale.

In this paper, the zone centre soft mode of KLT is investigated by hyper-Raman (HRM) spectroscopy as a function of temperature T in the interval from 10 to 200 K for $x = 0.011$, 0.0016, and 0.036. Besides the soft-mode frequency $\Omega_0(x, T)$ and damping constant $\gamma(x, T)$, the hyper-Rayleigh (HRL) intensity $I_{HRL}(x, T)$ is obtained, a relative calibration

being achieved by referring $I_{HRL}(x, T)$ to the integrated soft-mode HRM intensity of the same sample at high temperatures which is expected to be nearly independent of x.

As is well known, the soft mode does not trigger the dynamics of the phase or glass transition of KLT. This seems to be the reason why the detailed behaviour of $\Omega_0(x, T)$ and $\gamma(x, T)$ has more or less been ignored. For $x = 0.017$ Kamitakahara *et al* [21] have determined $\Omega_0(x, T)$ by inelastic neutron scattering at four temperatures below 100 K and have found a stiffening of the soft mode due to the presence of Li. The same conclusion has been drawn by Prater *et al* [22] from impurity-induced first-order features in the Raman spectrum of KLT. To the best of our knowledge, no quantitative information about $\gamma(x, T)$ with $x > 0$ is available from the literature.

As long as the polarization clusters around the Li ions are the source of both non-forward HRL scattering and SHG in or near the direction of the incident laser beam, both kinds of experiment should yield similar results. Previous SHG studies [16, 23], however, have been restricted in their dynamic range and therefore have not shown how the correlation between the polarization clusters evolves on approaching the freezing or phase transition temperature from above. Our HRM spectrometer enables us to pursue the increase of $I_{HRL}(x, T)$ for $T \to 0$ over five orders of magnitude and to determine the temperature at which $I_{HRL}(x, T)$ starts to deviate from its asymptotic behaviour in the limit of isolated polarization clusters and thus indicates the onset of impurity interaction.

Before proceeding to KLT, the present author has studied the influence of unavoidable, yet unidentified symmetry breaking defects, either extrinsic or intrinsic, in nominally pure $KTaO_3$ ($x = 0$) on $I_{HRL}(0, T)$, $\Omega_0(0, T)$, and $\gamma(0, T)$ [24–26]. Considerable variations of all three quantities were observed from sample to sample at a given temperature exceeding clearly the experimental errors at $T < 50$ K. The variations turned out to be correlated to each other and to the variation of the intensity of the defect-induced first-order Raman line of the zone centre transverse optic phonon around 545 cm^{-1}. In order to explain these findings, the defect cores were assumed to be surrounded by static or quasistatic lattice distortions dominated by the eigenvector of the soft mode. Accordingly, the size of these polarization clusters was characterized by the correlation radius r_c of the soft-mode polarization increasing for $T \to 0$ proportionally to the inverse of $\Omega_0(0, T)$. A similar model has been developed by Prusseit-Elffroth and Schwabl for explaining SHG in paraelectric perovskites [27].

The success achieved for nominally pure $KTaO_3$ suggests treating KLT in the same way as an ideal case where the symmetry breaking defects are known and their concentration is well controlled. If feasible at all, such an extrapolation has to be done with care and requires some discussion of the partly conflicting ideas conceived so far about the polarization clusters and the role of the soft mode in their formation.

The outline of this paper is as follows. In section 2 we describe experimental details and display our experimental results. The concepts used in interpreting our data are summarized in section 3. The discussion in section 4 is divided into three subsections dealing with $I_{HRL}(x, T)$, $\Omega_0(x, T)$, and $\gamma(x, T)$, respectively.

2. Experimental details and results

Measurements are carried out on single-crystal specimens of KLT grown from a slowly cooled molten solution of Ta_2O_5, K_2CO_3, and Li_2CO_3 by the self-nucleation technique [28, 29]. The samples under study are platelets of 1 to 6 mm edge lengths and are pieces of larger ingots the growth conditions of which are listed in [29] and referred to as KSK11, KSK18, and KSK25. The small sample thicknesses do not permit the observation of 90°

scattering from the bulk. Therefore we have to choose a near-backscattering configuration approximately specified by $x(yy)\bar{x}$ where x and y stand for two of the crystallographic axes. The backscattering configuration suffers from the superposition of proper HRL scattering from the bulk and SHG due to the lack of inversion symmetry at the sample surface [24]. In order to reduce the influence of surface SHG, the direction of geometrical reflections is blocked. We then succeed in recording HRM spectra of the KLT samples which at the upper end of the temperature interval under study become almost identical with the HRM spectrum of nominally pure $KTaO_3$ in the 90° scattering geometry $x(yy)z$ where z denotes the third of the cubic axes. Only the ratios of HRL and soft-mode HRM scattering intensities differ appreciably, but by factors reflecting the variations in the concentration of symmetry breaking defects. For this reason, we believe that the strength of the HRL line appearing in our HRM backscattering spectra mainly presents a bulk property and indicates the evanescence of inversion symmetry within the bulk of KLT for $T \to 0$.

Samples are mounted on a copper block in a continuous-flow cryostat and cooled by helium exchange gas. Their temperature is measured by means of a platinum resistor and kept constant within ±0.1 K. Heating by the laser radiation is avoided by passing the transmitted laser beam through a small hole in the copper block behind the sample. Details of the HRM spectrometer are described elsewhere [24]. The source of the exciting radiation is a Kr-lamp-pumped, acousto-optically Q-switched Nd-YAG laser with a pulse repetition rate of 5 kHz and an average power between 1 and 2 W at the location of the sample.

Typical results are shown in figure 1. The upper spectrum is obtained by combining the first stage of a double monochromator as a spectrograph and a position sensing photomultiplier tube (ITT-F4146 M, Mepsicron) as an optical multichannel detector. These devices can no longer be used in the temperature region of the glass or ferroelectric state because their dynamic range becomes too small for coping with the ratios of HRL and soft-mode HRM intensities. Therefore the lower spectrum is taken in the conventional manner combining both stages of a double monochromator and a photomultiplier tube (Burle/RCA C 31034) as an optical single-channel detector. With the spectrometer scanning through the HRL line, the intensity at its entrance slit is attenuated by calibrated neutral density filters.

For all Li concentrations x and temperatures T, the Stokes part of the HRM spectrum below 150 cm^{-1} is well described by the spectral function

$$S(\Omega, x, T) = I_{HRL}(x, T)\delta(\Omega) + \frac{2}{\pi}[n(\Omega, T) + 1]\, I_{HRM}(x, T) \times \frac{\Omega_0(x, T)\gamma(x, T)\Omega}{\left[\Omega_0^2(x, T) - \Omega^2\right]^2 + \gamma^2(x, T)\Omega^2} \tag{2}$$

where Ω is the HRM shift, i.e., the wavenumber shift from the second harmonic of the incident laser radiation, and $n(\Omega, T)$ the Bose–Einstein thermal population factor. The HRL intensity $I_{HRL}(x, T)$, the soft-mode frequency $\Omega_0(x, T)$, and the soft-mode damping constant $\gamma(x, T)$ have already been introduced in the preceding section. The intensity parameter $I_{HRM}(x, T)$ is, at least for $\gamma \ll \Omega_0$, the integral over the soft-mode HRM line after division by the thermal population factor. The convolution of equation (2) with the instrumental profile is fitted to the experimental data. Since the spectrum of hopping rates of the Li dipoles covers a frequency range below 1 GHz, the broadening of the HRL line due to the relaxation dynamics of the Li subsystem cannot be observed with the present set-ups, so that the measured HRL lineshape always coincides with the instrumental profile and a δ function has to be used in equation (2). The solid curves in figure 1 demonstrate the quality of our fitting procedure.

The soft-mode frequency $\Omega_0(x, T)$ and damping constant $\gamma(x, T)$ deduced from the

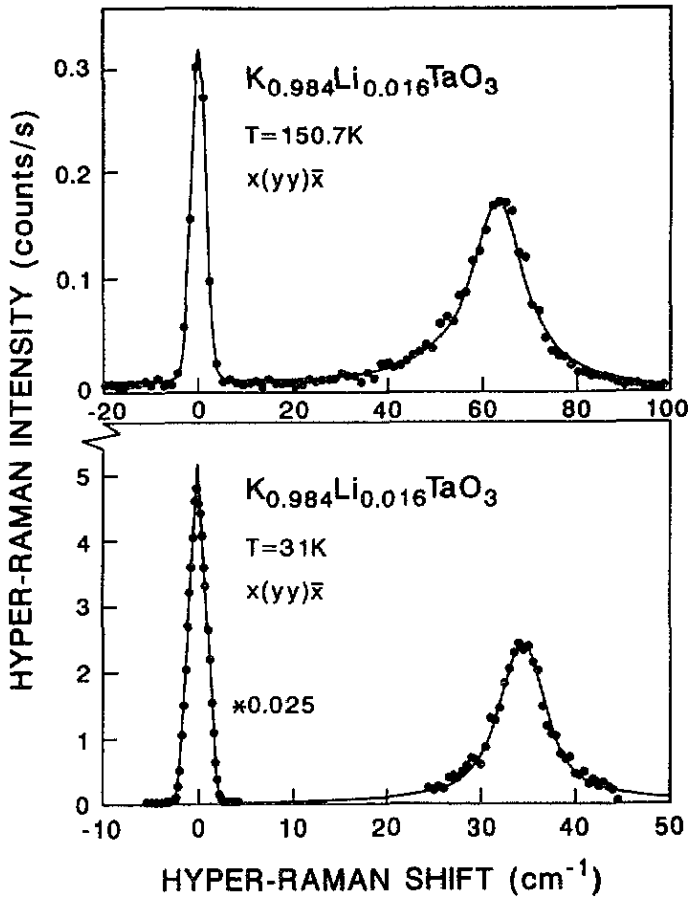

Figure 1. Stokes part of the low-frequency hyper-Raman spectrum of $K_{1-x}Li_xTaO_3$ with $x = 0.016$ at two different temperatures. The spectral resolution is indicated by the width of the hyper-Rayleigh line. The amplification factor of 0.025 in the lower diagram means that the hyper-Rayleigh line has been scaled down by a factor of 40. The hyper-Raman intensities in the two diagrams are not directly comparable because they refer to different spectrometer set-ups (see section 2).

HRM spectra are plotted as functions of temperature in figures 2 and 3, respectively. The data are supplemented by $\Omega_0(0, T)$ and $\gamma(0, T)$ taken from [26, 30]. As shown by the full lines in figure 2, $\Omega_0(x, T)$ turns out to follow Barrett's formula commonly used to describe the temperature dependence of the static dielectric constant or the square of the soft-mode frequency in the case of undoped $KTaO_3$ and $SrTiO_3$ [30, 31, 32]. Defining the four parameters T_1, T_0, $\tilde{\lambda}$, and $\Omega_0(\infty)$ of Barrett's formula as discussed in [30], we write

$$\Omega_0(T) = \frac{\Omega_0(\infty)\hat{\Omega}_0(T)}{\left[\Omega_0^2(\infty) + \hat{\Omega}_0^2(T)\right]^{1/2}} \tag{3a}$$

$$\hat{\Omega}_0^2(T) = 6\tilde{\lambda}\left(\frac{k_B T_1}{\hbar}\right)^2 \left\{\coth\left(\frac{T_1}{2T}\right) - \frac{2T_0}{T_1}\right\}. \tag{3b}$$

Fitting equations (3*a*) and (3*b*) to the experimental values of $\Omega_0(x, T)$, we obtain the x dependence of the four parameters listed in table 1. Since the theoretical foundation

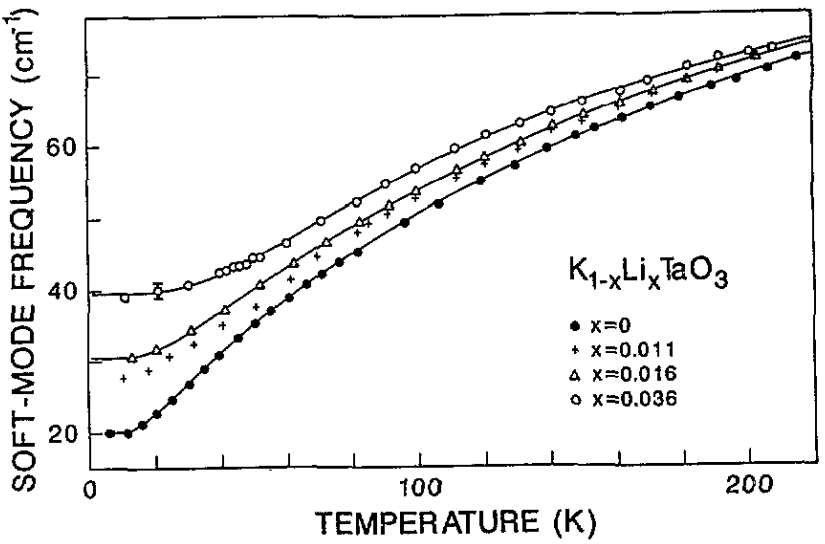

Figure 2. Temperature dependence of the soft-mode frequency $\Omega_0(x, T)$ of $K_{1-x}Li_xTaO_3$ including nominally pure $KTaO_3$. The solid lines are fits of Barrett's four-parameter formula to the experimental data.

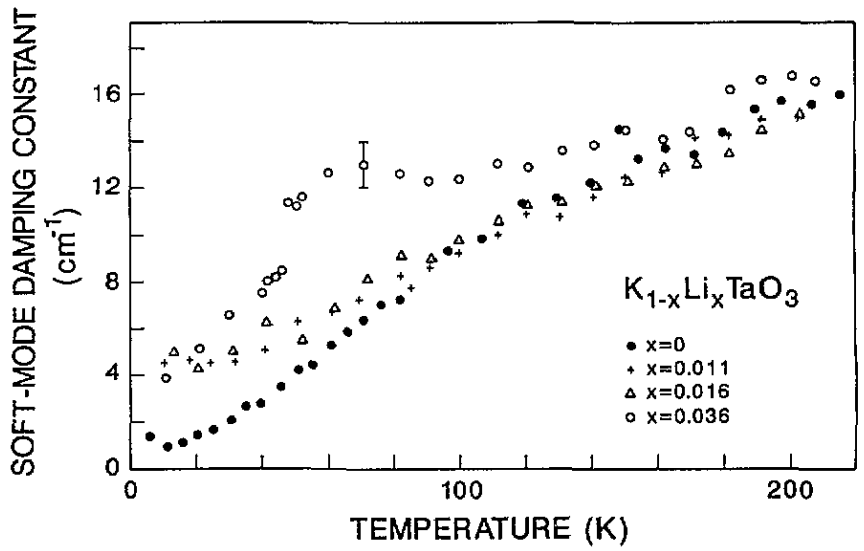

Figure 3. Temperature dependence of the soft-mode damping constant $\gamma(x, T)$ of $K_{1-x}Li_xTaO_3$ including nominally pure $KTaO_3$.

of Barrett's formula suffers from several inconsistencies [30], we shall neither dwell on explaining the physical meaning of the parameters nor base our discussion of the soft-mode stiffening on their x dependence. Instead, we consider equations (3*a*) and (3*b*) as a convenient interpolation formula for handling the experimental data.

Even for $x = 0.036$ no splitting of the soft mode due to a non-cubic crystal symmetry associated with the condensation of the Li subsystem is detectable. If it exists, it should be smaller than 3 cm^{-1}, provided the components appear with intensities of the same order

Table 1. The x dependence of the four parameters of Barrett's formula, equations (3*a*) and (3*b*), fitted to $\Omega_0(x, T)$.

x	T_1 (K)	T_0 (K)	$\bar{\lambda}$	Ω_∞ (cm^{-1})
0	55	14.4	0.10	162
0.011	76	15.4	0.082	144
0.016	85	15.6	0.077	138
0.036	120	22.7	0.067	118

of magnitude. One may argue that the observed Li-induced increase of $\gamma(x, T)$ at low temperatures mainly results from an unresolved splitting of the soft mode. In this case, however, it should be considerably larger for $x = 0.036$ than for $x = 0.011$ in contrast to the experimental data of figure 3.

The temperature dependence of the HRL intensity $I_{HRL}(x, T)$ is shown in figure 4. In order to reduce the experimental errors, the data of figure 4 are not taken from the fits of equation (2) to the HRM spectra, but are determined in additional continuous runs at constant laser intensity. At each temperature the samples are given about 15 min to relax to thermal equilibrium before the HRL photon counts are accumulated. Using calibrated neutral density filters in front of the entrance slit of the spectrometer, we can easily extend the dynamic range of $I_{HRL}(x, T)$ to five orders of magnitude without changing any other experimental condition. For $x = 0.011$ and 0.016 stepwise cooling yields the same temperature behaviour of $I_{HRL}(x, T)$ as stepwise heating, whereas for $x = 0.036$ a pronounced thermal hysteresis with rather steep edges is observed around 50 K as indicated by the open and solid circles in the top diagram of figure 4. Assuming the integrated intensity of the soft-mode HRM line to become almost independent of x at high temperatures, we can calibrate the HRL intensities by referring them to the soft-mode HRM intensity of the same sample at 200 K. For this purpose, the intensity scales of the two lower diagrams of figure 4 are corrected by the factors

$$c(x) = \frac{I_{HRL}(x_r, T_r)}{I_{HRL}(x, T_r)} \left(\frac{I_{HRL}}{I_{HRM}}\right)_{x,T_r} \left(\frac{I_{HRM}}{I_{HRL}}\right)_{x_r,T_r} \tag{4}$$

with $x_r = 0.036$ and $T_r = 200$ K, the ratios I_{HRL}/I_{HRM} being available from the fits of equation (2) to the HRM spectra measured at 200 K.

The occurrence of a thermal hysteresis in $I_{HRL}(x, T)$ for $x = 0.036$ is a stimulus to look more closely for a similar effect in $\Omega_0(x, T)$ and $\gamma(x, T)$. As long as we have to resort to single-channel recording of the HRM spectra in the relevant temperature range, however, complete cooling and heating cycles become extremely time consuming. Therefore we have to confine ourselves to measuring the soft-mode HRM line at some temperatures within the hysteresis interval after slowly cooling from about 100 K on the one hand and slowly heating from about 20 K on the other hand. No difference is found for $\Omega_0(x, T)$ within the limits of experimental accuracy, whereas $\gamma(x, T)$ varies by more than 2 cm^{-1}. We conclude that the thermal hysteresis in $I_{HRL}(x, T)$ is accompanied by a similar one in $\gamma(x, T)$, in accordance with the general observation that in passing from $x = 0.016$ to $x = 0.036$ both $I_{HRL}(x, T)$ and $\gamma(x, T)$ change their character as functions of temperature while $\Omega_0(x, T)$ does not exhibit new features.

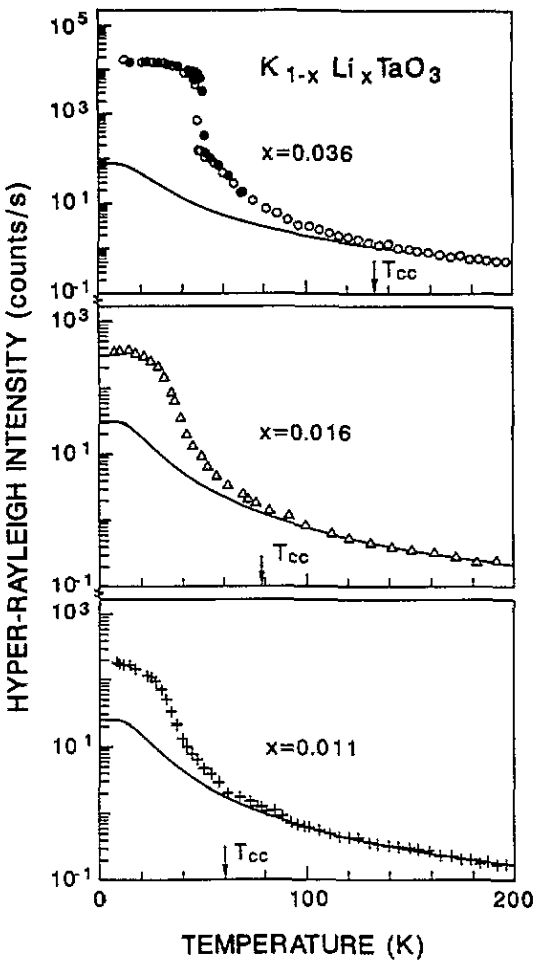

Figure 4. Temperature dependence of the hyper-Rayleigh intensity $I_{HRL}(x, T)$ of $K_{1-x}Li_xTaO_3$. Crosses, triangles, and open circles refer to cooling, full circles to heating. Thermal hysteresis is only observed for $x = 0.036$. The solid lines describe the asymptotic behaviour in the limit of uncorrelated polarization clusters. T_{cc} is the cluster coalescence temperature defined by the condition $ax^{-1/3} = 2r_c(0, T_{cc})$ (see section 3).

3. The polarization cluster concept

The coupling between the Li dipoles and the $KTaO_3$ host lattice is a problem still under controversial discussion, especially with regard to the role of the zone centre soft mode [1, 2, 12–14, 16]. Since in pure $KTaO_3$ the K ions do not participate appreciably in the soft-mode vibration, one may argue that a soft-mode-type quasistatic lattice distortion leaves a Li dipole at the K site almost unaffected and, vice versa, a Li dipole cannot induce a significant soft-mode polarization. Indeed, the electrostatic Li–soft-mode interaction appears to be absent by symmetry if only point dipoles at the ideal lattice sites are considered and the soft mode is reduced to a vibration of the central Ta ion against the rigid oxygen cage [16]. On the other hand, Vugmeister and Glinchuk [1, 33] have based their model of ferroelectric ordering in KLT on the potential energy of a Li point dipole embedded in the effective or exciting electric field [34] due to the Li-induced host lattice polarization. Despite the

symmetry argument just quoted, the effective electric field at the Li site arising from the soft-mode polarization does not vanish because of the Lorentz term $\Gamma \boldsymbol{P}$, the Lorentz factor Γ deviating from $4\pi/3$ insofar as the displacement pattern of the soft mode includes a distortion of the oxygen octahedron. It has been pointed out, however, that a non-vanishing Lorentz term implies some Li–soft-mode interaction to exist *a priori* [14]. This interaction has been introduced by Vugmeister and Glinchuk only globally in the form

$$\boldsymbol{P}^{SM}(\boldsymbol{q}) \sim \left[\frac{Z^T}{\Omega(\boldsymbol{q})}\right]^2 \Gamma \frac{\langle p_{\mathrm{Li}}\rangle}{v} \tag{5}$$

where $\boldsymbol{P}^{SM}(\boldsymbol{q})$ is the Fourier component of the soft-mode polarization belonging to the wavevector $\boldsymbol{q}$, $\langle p_{\mathrm{Li}}\rangle$ an appropriate statistical average of an individual Li dipole moment, v the volume of the unit cell, and $\Omega(\boldsymbol{q})$ the dispersion relation of the soft-mode phonon branch for small wavevectors. Usually, this dispersion is described by [24]

$$\Omega^2(\boldsymbol{q}) = \Omega_0^2 + D^2\left(\frac{\boldsymbol{q}}{q}\right)q^2 \tag{6}$$

with an anisotropic coefficient D depending on the wavevector direction. Although the model based on equations (5) and (6) provides a self-consistent description of a soft-mode-mediated electrostatic interaction between Li dipoles, it does not give a detailed account of the Li–soft-mode coupling which certainly involves both Coulomb and short-range forces.

One of the main obstacles to a more rigorous treatment of this problem is the large off-centre displacement δ of the Li ion (around a quarter of the lattice constant) provoking a strongly anharmonic reaction of the host crystal environment to which the concepts and symmetry arguments pertinent to an undisturbed harmonic lattice no longer apply [3]. For this reason we confine ourselves to the simpler question of to what extent the lattice distortions around the Li ions may be characterized as 'frozen-in' soft mode.

Some experimental answer is given by the observation [16, 23] that SHG in KLT is well described in terms of the fourth-rank tensor determining electric-field-induced SHG (ESHG) in pure $KTaO_3$. According to [35], the components of this tensor referred to the cubic axes may be expanded in the following way (cgs units):

$$\frac{\partial \chi^{(2)}_{ijk}}{\partial E_l} = \sum_{\sigma} \frac{\partial \chi^{(2)}_{ijk}}{\partial P^{\sigma}_l}\frac{\Delta\varepsilon_{\sigma}(0)}{4\pi} + \left[\frac{\partial \chi^{(2)}_{ijk}}{\partial E_l}\right]_{\text{all } P^{\sigma}=0}. \tag{7}$$

Here, $\chi^{(2)}$ is the second-order or SHG susceptibility, $\boldsymbol{E}$ the externally applied electric field, $\boldsymbol{P}^{\sigma}$ the lattice polarization associated with the infrared active phonon σ, and $\Delta\varepsilon_{\sigma}(0)$ the contribution of this phonon to the static dielectric constant $\varepsilon(0)$ of $KTaO_3$. The term outside the sum over σ is of purely electronic origin and may be identified with the optical third-order susceptibility. As can be inferred from the large soft-mode contribution $\Delta\varepsilon_{\mathrm{SM}}(0)$ to $\varepsilon(0)$, an external electric field mainly induces the displacement pattern of the soft mode, so that expansion (7) reduces to

$$\frac{\partial \chi^{(2)}_{ijk}}{\partial E_l} \approx \frac{\Delta\varepsilon_{\mathrm{SM}}(0)}{4\pi}\frac{\partial \chi^{(2)}_{ijk}}{\partial P^{\mathrm{SM}}_l} = \frac{Z^T}{\Omega_0^2}\frac{\partial \chi^{(2)}_{ijk}}{\partial Q^{\mathrm{SM}}_l} \tag{8}$$

where Q^{SM}_l is the normal coordinate giving rise to the soft-mode polarization P^{SM}_l in the direction of the lth cubic axis and the definitions of [35, 36] are used including a mass factor in both the normal coordinate and the transverse effective charge. Since the derivative of $\chi^{(2)}$ with respect to Q^{SM} is the HRM tensor of the soft mode, SHG in KLT is not only related to ESHG in $KTaO_3$, but to soft-mode HRM scattering in $KTaO_3$ as well. In fact,

it has been confirmed experimentally [23, 35] that the tensors underlying the three effects approximately agree in all ratios of their components, e.g.

$$\left(\frac{\partial\chi^{(2)}_{333}/\partial Q^{SM}_3}{\partial\chi^{(2)}_{311}/\partial Q^{SM}_3}\right)^2_{KTaO_3} \approx \left(\frac{\partial\chi^{(2)}_{333}/\partial E_3}{\partial\chi^{(2)}_{311}/\partial E_3}\right)^2_{KTaO_3} \approx \left(\frac{d_{333}}{d_{311}}\right)^2_{KLT} \approx 6 \tag{9}$$

where d_{333} and d_{311} denote SHG tensor components of a single polarization cluster polarized in the z direction.

The results just discussed support two assumptions:

(a) SHG in KLT reflects the nonlinear optical response of the $KTaO_3$ host crystal having lost its inversion symmetry by local distortions.

(b) The soft-mode eigenvector dominates the Li-induced lattice distortions of small wavevectors q.

Admittedly, no conclusions can be drawn about elastic strains because they do not couple to $\chi^{(2)}$. We note, however, that their presence should influence the Li-induced birefringence via the photoelastic effect. To the best of our knowledge, birefringence data of KLT have always been amenable to an interpretation in terms of the quadratic electro-optic effect under neglect of non-electrostrictive strains and the linear photoelastic effect due to them [15, 1]. Therefore we regard Li-induced elastic strains to be of minor importance in comparison to the Li-induced soft-mode polarization.

As long as the polarization clusters can be considered as isolated, it is tempting to apply the model of [24, 25, 27] and to distinguish between a defect core and an outer range in which the soft-mode polarization decays according to the Ornstein–Zernike function, i.e.

$$P^{SM}(r) \sim \frac{1}{r}\exp\left\{-\frac{r}{r_c}\right\} \tag{10}$$

where r_c is the correlation radius given by

$$r_c = \frac{D}{\Omega_0}. \tag{11}$$

The coefficient D is an appropriate average of $D(q/q)$ introduced by equation (6). It is assumed to be independent of temperature, so that r_c varies with temperature as the inverse of the soft-mode frequency.

In a naive picture, the polarization clusters cease to be independent of each other and start to coalesce as soon as they touch each other. Accordingly, we may define a cluster coalescence temperature $T_{cc}(x)$ by the condition that the mean distance between adjacent Li ions equals twice the correlation radius, i.e.

$$d = 2r_c(T_{cc}) \tag{12a}$$

with

$$d = \frac{a}{x^{1/3}} \tag{12b}$$

where a is the lattice constant. Inserting the low-temperature limit $r_c(0) \approx 18$ Å [23, 24, 27] in equations (12*a*) and (12*b*), we find that the concept of isolated polarization clusters always breaks down below a certain temperature if the Li concentration x exceeds a threshold of about 0.13%. Conversely, this value justifies neglecting the interaction of polarization clusters in nominally pure $KTaO_3$ because the molar concentration of the responsible defects is certainly less [23, 24, 27].

The solid line in figure 5 presents T_{cc} as a function of x according to equations (11), (12*a*), and (12*b*). The dashed line is obtained by replacing the soft-mode frequency of pure $KTaO_3$, i.e. $\Omega_0(0, T)$ in the notation of section 2, by the soft-mode frequency $\Omega_0(x, T)$ of KLT. Barrett's formula (equations (3*a*) and (3*b*)) and interpolating second-degree polynomials for describing the x dependence of its four parameters are used. As doping with Li reduces the correlation radius at a given temperature, the 'renormalized' values of $T_{cc}(x)$ become smaller than those obtained before.

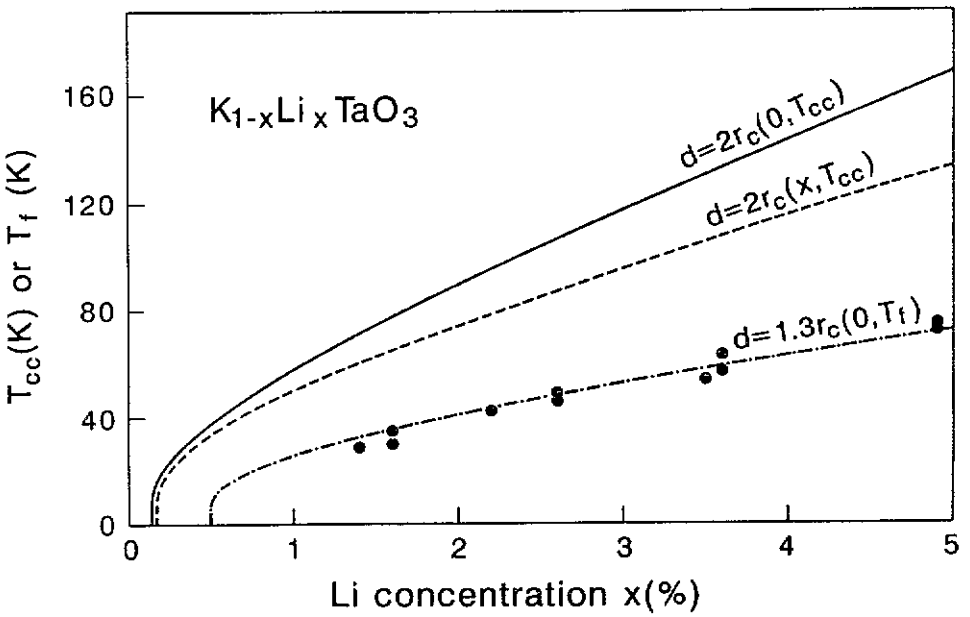

Figure 5. Cluster coalescence temperature T_{cc} and freezing temperature T_f of $K_{1-x}Li_xTaO_3$ as functions of the Li concentration x. d = mean distance between adjacent Li ions, $r_c(x, T)$ = correlation radius of the soft-mode polarization as a function of both Li concentration and temperature. Solid line: $T_{cc}(x)$ according to $d = 2r_c(0, T_{cc})$; dashed line: $T_{cc}(x)$ according to $d = 2r_c(x, T_{cc})$; full circles: experimentally determined freezing temperature $T_f(x)$ taken from [5]; dashed–dotted line: $T_f(x)$ according to $d = 1.3r_c(0, T_f)$. The factor of 1.3 is the result of a fit to the experimental points.

In view of the blurred boundary of a polarization cluster, the factor of two in equation (12*a*) is quite arbitrary. Replacing it by an adjustable parameter, we try to reproduce the x dependence of the experimentally determined freezing temperature T_f [5]. The result is shown by the dashed–dotted line in figure 5. If $\Omega_0(x, T)$ is used instead of $\Omega_0(0, T)$, the prefactor of $r_c(T_f)$ in equation (12*a*) increases from 1.3 to 1.6, the quality of the fit being the same. Although such an extrapolation of equation (12*a*) down to T_f is an oversimplification, it seems to reveal two relevant features.

(a) Above T_f, the outer range of each polarization cluster expands with decreasing temperature.

(b) Steric hindrance triggers the onset of interaction between the polarization clusters.

It is left to the following section to show how far the concept of a cluster coalescence temperature is supported by our experimental data.

4. Interpretation of experimental results

4.1. Temperature dependence of the hyper-Rayleigh intensity

As explained in [24, 25], HRL scattering from nominally pure $KTaO_3$ is mainly determined by three factors, i.e. the concentration of the relevant defects, the fourth power of the reciprocal soft-mode frequency, and the square of the soft-mode polarization at the defect core. Applying the underlying ideas to KLT, we expect the asymptotic law

$$I_{\mathrm{HRL}}(x, T) \sim x\Omega_0^{-4}(0, T) \tag{13}$$

to hold at sufficiently high temperatures where the Li-induced polarization clusters may be considered as independent and describable in terms of an Ornstein–Zernike function. We do not insert $\Omega_0(x, T)$ in equation (13), because there is no reason to believe that the approximation of next-higher order is obtained in this way. The solid lines in figure 4 represent extrapolations of $I_{\mathrm{HRL}}(x, T)$ from the upper portion of the temperature interval under study to lower temperature according to equation (13). Within the limits of experimental accuracy, we find $I_{\mathrm{HRL}}(x, T)$ to be proportional to x for $T > 150$ K. Moreover, $I_{\mathrm{HRL}}(x, T)$ starts to deviate from its asymptotic behaviour around the cluster coalescence temperature T_{cc} defined by equations (12*a*) and (12*b*) and indicated by arrows in figure 4.

Below T_{cc}, $I_{\mathrm{HRL}}(x, T)$ increases with decreasing temperature much more rapidly than $\Omega_0^{-4}(0, T)$ because the polarization clusters combine and the reduction in the number of scattering centres is overcompensated by the growth of the intensity each scattering centre contributes to $I_{\mathrm{HRL}}(x, T)$. We may evaluate the correlation radius $\xi_c(x, 0)$ of the Li-induced soft-mode polarization in the low-temperature limit by

$$\xi_c(x, 0) \approx \frac{d(x)}{2}\left[\frac{I_{\mathrm{HRL}}(x, 0)}{I_{\mathrm{HRL}}(x, T_{cc})}\right]^{1/3}. \tag{14}$$

Here, we use the idea that a coalescence of every N polarization clusters to one, let us say, ferroelectric microdomain divides the number of scattering centres by N, but enlarges the intensity contribution of each of them by a factor of N^2 because the scattered wavelets add coherently within the single polarization clusters or microdomain provided its diameter remains small compared to the wavelength $\lambda = 532$ nm of the scattered light [24]. As a result, the ratio $I_{\mathrm{HRL}}(x, 0)/I_{\mathrm{HRL}}(x, T_{cc})$ measures the volume expansion of the polarization clusters due to coalescence or the number of Li impurities covered by a microdomain at low temperatures. Estimating this number by $\left[\xi_c(x, 0)/(d/2)\right]^3$, we obtain equation (14). In table 2 we have listed d, T_{cc}, and $\xi_c(x, 0)$ according to equation (14) as functions of x. Our values of $\xi_c(x, 0)$ are consistent with the condition $\xi_c(x, 0) \ll \lambda$ and in remarkable agreement with those of [16] deduced from SHG data by an entirely different procedure.

Table 2. The mean distance d between adjacent Li ions, the cluster coalescence temperature T_{cc}, and the low-temperature correlation radius $\xi_c(x, 0)$ as functions of the Li concentration x.

			$\xi_c(x, 0)$ (nm)		
x	d (Å)	T_{cc} (K)	Equation (14)	[16]	[23]
0.011	18	62	4		
0.016	16	78	5	6	14
0.036	12	130	15	12 (x = 0.034)	140

Nevertheless, we must point out that we have tacitly assumed the scattering process to remain incoherent at all temperatures and Li concentrations, so that $I_{HRL}(x, T)$ is always the sum of the intensities scattered by uncorrelated polarization clusters or microdomains. If we suppose the scattering process to become coherent at low temperatures, we have to postulate that the ensemble of microdomains is ordered in such a way that it has an appreciable structure factor at the scattering wavevector q. This is only possible if $\xi_c(x, 0)$ reaches the order of magnitude of $2\pi/q$. For our backscattering configuration, we find

$$\frac{2\pi}{q} = \frac{\lambda}{[n(\lambda) + n(2\lambda)]} \approx 120 \text{ nm} \tag{15}$$

where $n(\lambda)$ and $n(2\lambda)$ are the refractive indices at the second-harmonic and laser wavelength, respectively. As quoted in table 2, a value $\xi_c(x, 0) = 140$ nm already for $x = 0.036$ has been estimated in [23]. There the appearance of distinct lateral peaks in the angular distribution of the second-harmonic intensity has been reported and interpreted as evidence of such a large value of $\xi_c(x, 0)$. If the estimates of $\xi_c(x, 0)$ in [23] were correct, the jumps in $I_{HRL}(x, T)$ observed for $x = 0.036$ would be accompanied by a transition from incoherent to coherent scattering of second-harmonic light or vice versa. According to [16], however, the scattered second-harmonic intensity remains rather uniformly distributed in a cone of at least 30° around the direction of the incident laser beam up to $x = 0.06$. As will be explained in section 4.3, the absence of any soft-mode splitting even for $x = 0.036$ is an argument in favour of equation (14), the small values of $\xi_c(x, 0)$, and HRL scattering in the strict sense. Of course, a superposition of coherent and incoherent contributions to the elastic scattering of second-harmonic light cannot be ruled out.

4.2. Temperature dependence of the soft-mode frequency

A variety of mechanisms can be imagined to contribute to the shift of the soft-mode frequency in the presence of defect-induced lattice distortions. Neglecting elastic strains as in section 3, we concentrate on the three mechanisms discussed in [25].

(a) As verified experimentally by application of an external electric field [37], a static or quasistatic homogeneous lattice polarization stiffens the soft mode of $KTaO_3$. This effect is characterized by

$$\left[\Omega_0^2(P^{SM}, T) - \Omega_0^2(0, T)\right] \sim \left(P^{SM}\right)^2 \tag{16}$$

where the superscript SM indicates that an external electric field mainly gives rise to the displacement pattern of the soft mode. Interpreted in terms of a simple model, equation (16) describes the frequency shift of an anharmonic oscillator biased by a static external force. Applying equation (16) to KLT, we have to replace the right-hand side by the spatial average of the square of the Li-induced soft-mode polarization. In the limit of independent polarization clusters, we expect an asymptotic behaviour of the soft-mode frequency shift in the form [25]

$$\Delta^{(a)}\Omega_0(x, T) \sim \frac{\left\langle\left[P^{SM}(r)\right]^2\right\rangle}{\Omega_0(0, T)} \sim \frac{x}{\Omega_0(0, T)}\left\{\frac{1}{\Omega_0(0, T)} + C\right\}. \tag{17}$$

In the last bracket we have added the constant term C in order to take into account not only the outer ranges of the polarization clusters as described by equation (10), but also the defect cores which may be rather large because of $\delta \approx 0.25a$. An analogous constant term in equation (13) turns out to be almost negligible because of the rapid growth of $\Omega_0^{-4}(0, T)$ for $T \to 0$.

(b) The Li-induced reduction of symmetry opens new channels for multiphonon processes contributing to both damping and frequency shift of the soft mode. Confining attention to the two-phonon decay of the soft mode, we find that in the limit of independent polarization clusters the soft-mode frequency shift is given in a coarse approximation by [25]

$$\left|\Delta^{(b)}\Omega_0(x,T)\right| \sim \frac{x}{\Omega_0(0,T)}. \tag{18}$$

While $\Delta^{(a)}\Omega_0(x,T)$ is always positive, $\Delta^{(b)}\Omega_0(x,T)$ can be negative.

(c) Scattering by polarization clusters provides an additional coupling between the phonons of the soft-mode branch. The resulting soft-mode frequency shift follows the asymptotic law [25]

$$\left|\Delta^{(c)}\Omega_0(x,T)\right| \sim \frac{x^2}{\Omega_0^6(0,T)}. \tag{19}$$

In figure 6 we have plotted the Li-induced frequency shift $\Delta\Omega_0(x,T) = \Omega_0(x,T) - \Omega_0(0,T)$ as a function of temperature. The solid lines represent fits of the expression

$$\Delta\Omega_0(x,T) = \frac{A_1(x)}{\Omega_0(0,T)} + \frac{A_2(x)}{\Omega_0^2(0,T)} \tag{20}$$

to the experimental points. The coefficients $A_1(x)$ and $A_2(x)$ turn out to be approximately linear with x, so that our results seem to support equations (17) and (18), i.e. a superposition of mechanisms (a) and (b). We note, however, that equations (17) and (18) only refer to the case of independent polarization clusters as well as small frequency shifts and that there is no evident reason why they should hold below $T_{cc}(x)$ and for frequency shifts $\Delta\Omega_0(x,T)$ reaching the order of magnitude of $\Omega_0(0,T)$ itself. Provided that mechanism (a) is the only relevant one, we may argue that $\left\langle\left[P^{\mathrm{SM}}(r)\right]^2\right\rangle$ is insensitive to antiparallel alignments of polarization clusters and therefore monitors 'quadrupolar' [16] rather than dipolar long-range correlations. One can easily imagine a realignment of polarization clusters to larger units (microdomains) leaving $\left\langle\left[P^{\mathrm{SM}}(r)\right]^2\right\rangle$ nearly invariant. In addition, the *square* of $P^{\mathrm{SM}}(r)$ gives weight to the interior of the polarization clusters which, apart from flips into other directions of polarization, may be rather unaffected by the cluster coalescence. The two arguments just explained for $\left\langle\left[P^{\mathrm{SM}}(r)\right]^2\right\rangle$ also apply to higher-even-power terms like $\left\langle\left[P^{\mathrm{SM}}(r)\right]^4\right\rangle$ which have to be taken into account in equations (16) and (17) to make them usable even for large soft-mode frequency shifts. Thus we may understand why dramatic changes due to cluster coalescence as in $I_{\mathrm{HRL}}(x,T)$ are not observed in $\Delta\Omega_0(x,T)$.

In contrast to figure 6, the defect-induced shift of the soft-mode frequency of nominally pure $KTaO_3$ at 5 K was found to increase quadratically with the defect concentration as measured by the intensity of a defect-induced first-order Raman feature [25]. This result was therefore interpreted in terms of mechanism (c). The difference in the defect concentration dependence may indicate nothing more than the dominance of mechanisms (a) and (b) over (c) just in the special case of Li impurities. It may also underline that mechanism (c) is most effective near the M_0 critical point of the one-phonon density of states of the soft-mode branch and loses significance for large frequency shifts as it certainly does at elevated temperatures because of the high power of $\Omega_0(0,T)$ in the denominator of equation (19).

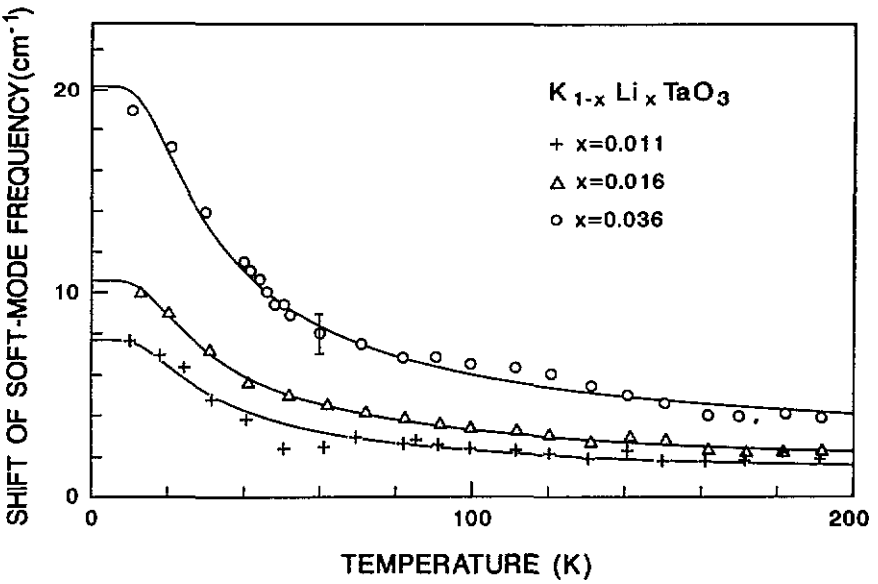

Figure 6. Li-induced shift $\Delta\Omega_0(x, T) = \Omega_0(x, T) - \Omega_0(0, T)$ of the soft-mode frequency of $K_{1-x}Li_xTaO_3$ as a function of temperature. The solid lines are fits of equation (20) to the experimental points.

4.3. Temperature dependence of the soft-mode damping constant

Treating equation (16) more exactly, we have to distinguish between the two cases in which the eigenvector of the soft mode is parallel and perpendicular to the Li-induced soft-mode polarization [37]. The presence of polarization clusters of various orientations may then lead to the conclusion that the soft-mode HRM line must split or at least broaden if the splitting cannot be resolved. The observation of this effect, however, requires the correlation radius $\xi_c(x, T)$ to have the order of magnitude of the reciprocal wavevector of the soft mode under study, i.e. $\xi_c(x, T) \approx 2\pi/q \approx 120$ nm according to equation (15). As shown by table 2, the low-temperature limit $\xi_c(x, 0)$ estimated by means of equation (14) remains much smaller than 120 nm, so that a splitting of the soft mode cannot be expected in agreement with our experimental findings described in section 2. On the other hand, $\xi_c(x, 0) \approx 140$ nm [23] would certainly result in an observable soft-mode splitting for $x = 0.036$. We may state that for soft-mode HRM scattering our KLT samples are still cubic despite cluster coalescence. Mechanism (a) does not give rise to a distribution of frequency shifts, but to a single value of $\Delta^{(a)}\Omega_0(x, T)$ determined by an appropriate average of equation (16). Of course, scattering techniques penetrating further into the Brillouin zone may detect a soft-mode splitting even for $x \leqslant 0.036$. Hence our result is not in contradiction to indications of tetragonal symmetry and corresponding mode splittings observed by neutron [38] and defect-induced first-order Raman scattering [22] for $2\pi/q \lesssim \xi_c(x, T)$.

Our arguments leave mechanism (b) as the main reason for the Li-induced increment $\Delta\gamma(x, T) = \gamma(x, T) - \gamma(0, T)$ of the damping constant. For $x = 0.011$ and 0.036 the temperature dependence of $\Delta\gamma(x, T)$ is similar to that obtained for the difference of the damping constant of $KTaO_3$ samples [26]. However, the increase of $\Delta\gamma(x, T)$ on cooling can no longer be accounted for by a mere expansion of the disturbed portion of the crystal because the Li-induced lattice distortions extend over the whole crystal below $T_{cc}(x)$. On the

contrary, there is the opposite trend to decrease $\Delta\gamma(x, T)$ by establishing a new crystalline long-range order via the coalescence of polarization clusters to microdomains. According to figure 3, the latter effect seems to become dominant for $x = 0.036$ below the temperature indicated by a jump of $I_{HRL}(x, T)$ and previously referred to as Curie temperature of a 'rounded first-order transition' [15].

5. Summary

HRM spectroscopy is applied to single crystals of KLT in order to determine the soft-mode frequency $\Omega_0(x, T)$, the soft-mode damping constant $\gamma(x, T)$, and the appropriately calibrated HRL intensity $I_{HRL}(x, T)$ as functions of Li concentration x and temperature T. The experimental results are amenable to an interpretation based on two assumptions.

(i) With regard to the three quantities under study KLT can be treated as locally distorted pure $KTaO_3$.

(ii) The small-wavevector Fourier components of the Li-induced lattice distortions are mainly soft-mode displacements. In this sense, each Li impurity is surrounded by a frozen-in soft mode. The contributions of elastic strains and of the eigenvectors of the other zone centre optical phonons are neglected.

HRL scattering turns out to be a sensitive tool for studying the evolution of dipolar correlation in KLT. Depending on the average of even powers of the Li-induced soft-mode polarization, the shift $\Delta\Omega_0(x, T) = \Omega_0(x, T) - \Omega_0(0, T)$ of the soft-mode frequency remains almost unaffected by the coalescence of polarization clusters. Up to $x = 0.036$ neither a splitting of the soft mode nor a broadening of the soft-mode HRM line due to an unresolved splitting is observed, in accordance with estimates of the dipolar correlation radius and the soft-mode wavevector involved in the HRM scattering process. Both $I_{HRL}(x, T)$ and $\gamma(x, T)$ support the conjecture of Kleemann *et al* [15] that the nature of the Li dipole condensation changes around $x_c \approx 0.022$.

The present work has to be continued to lower as well as higher Li concentrations. In the first case a closer connection to nominally pure $KTaO_3$ can be achieved, while in the second case a further evolution of tetragonal order can be studied.

Acknowledgments

The author is much indebted to D Rytz for generously providing the samples of KLT. He also thanks J Kuhl for a critical reading of the manuscript. The financial support of the Deutsche Forschungsgemeinschaft (Bonn, Germany) is gratefully acknowledged.

References

[1] Vugmeister B E and Glinchuk M 1990 *Rev. Mod. Phys.* **62** 993
[2] Höchli U T, Knorr K and Loidl A 1990 *Adv. Phys.* **39** 405
[3] Exner M, Catlow C R A, Donnerberg H and Schirmer O F 1994 *J. Phys.: Condens. Matter* **6** 3379
[4] Zhurova E A, Zavodnik V E, Ivanov S A, Syrnikov P P and Tsirelson V G 1993 *Z. Naturf.* a **48** 25
[5] van der Klink J J, Rytz D, Borsa F and Höchli U T 1983 *Phys. Rev.* B **27** 89
[6] Yacoby Y and Just S 1974 *Solid State Commun.* **15** 715
[7] Mahan G D 1967 *Phys. Rev.* **153** 983
[8] van der Klink J J and Khanna S N 1984 *Phys. Rev.* B **29** 2415
[9] Stachiotti M G and Migoni R L 1990 *J. Phys.: Condens. Matter* **2** 4341
[10] Höchli U T and Baeriswyl D 1979 *J. Phys. C: Solid State Phys.* **17** 311

[11] Höchli U T, Weibel H E and Boatner L A 1979 *J. Phys. C: Solid State Phys.* **12** L563
[12] Vugmeister B E, Glinchuk M D and Pechenyi A P 1984 *Sov. Phys.–Solid State* **26** 2036
[13] Stachiotti M G, Migoni R L and Höchli U T 1991 *J. Phys.: Condens. Matter* **3** 3689
[14] Höchli U T and Maglione M 1989 *J. Phys.: Condens. Matter* **1** 2241
[15] Kleemann W, Kütz S and Rytz D 1987 *Europhys. Lett.* **4** 239
[16] Azzini G A, Banfi G P, Guilotto E and Höchli U T 1991 *Phys. Rev.* B **43** 7473
[17] Di Antonio P, Vugmeister B E, Toulouse J and Boatner L A 1993 *Phys. Rev.* B **47** 5629
[18] Doussineau P, Farssi Y, Frénois C, Levelut A, McEnaney K, Toulouse J and Ziolkiewicz S 1993 *Europhys. Lett.* **24** 415
[19] Wickenhöfer F, Kleemann W and Rytz D 1991 *Ferroelectrics* **124** 237
[20] Doussineau P, Farssi Y, Frénois C, Levelut A, McEnaney K, Toulouse J and Ziolkiewicz S 1993 *Europhys. Lett.* **21** 323
[21] Kamitakahara W A, Loong C K, Ostrowski G E and Boatner L A 1987 *Phys. Rev.* B **35** 223
[22] Prater R L, Chase L L and Boatner L A 1981 *Phys. Rev.* B **23** 5904
[23] Voigt P and Kapphan S 1994 *J. Phys. Chem. Solids* **55** 853
[24] Vogt H 1990 *Phys. Rev.* B **41** 1184; 1990 *Ferroelectrics* **107** 79
[25] Vogt H 1991 *J. Phys.: Condens. Matter* **3** 3697
[26] Vogt H 1992 *Ferroelectrics* **125** 313
[27] Prusseit-Elffroth W and Schwabl F 1990 *Appl. Phys.* A **51** 361
[28] Samples were provided by D Rytz, Sandoz Huningue SA, Centre de Recherche en Optoelectronique, F-68330 Huningue, France.
[29] van der Klink J J and Rytz D 1982 *J. Cryst. Growth* **56** 673
[30] Vogt H 1995 *Phys. Rev.* B **51** 8046
[31] Lines M E and Glass A M 1979 *Principles and Applications of Ferroelectrics and Related Materials* (Oxford: Clarendon) p 253
[32] Müller K A and Burkard H 1979 *Phys. Rev.* B **19** 3593
[33] Vugmeister B E and Glinchuk M D 1980 *Sov. Phys.–JETP* **52** 482
[34] Born M and Huang K 1968 *Dynamical Theory of Crystal Lattices* (Oxford: Clarendon) pp 101, 253
[35] Vogt H 1987 *Phys. Rev.* B **36** 5001
[36] Vogt H 1988 *Phys. Rev.* B **38** 5699
[37] Fleury P A and Worlock J M 1968 *Phys. Rev.* **174** 613
[38] Toulouse J and Hennion B 1994 *Phys. Rev.* B **49** 1503